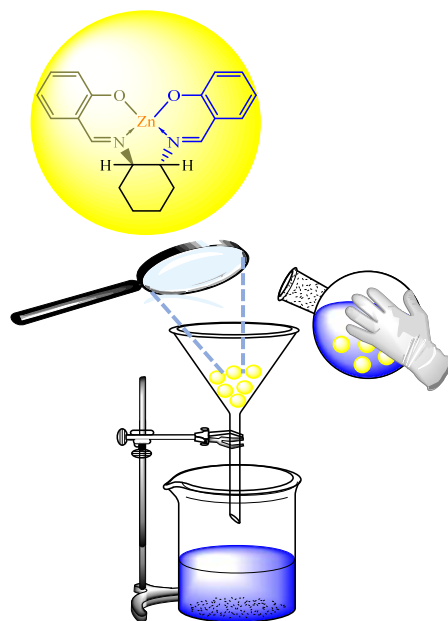


Chapter 5

Sustainable approach for the synthesis of chiral β -aminoketones using an encapsulated chiral Zn(II)–salen complex



5.1 Introduction

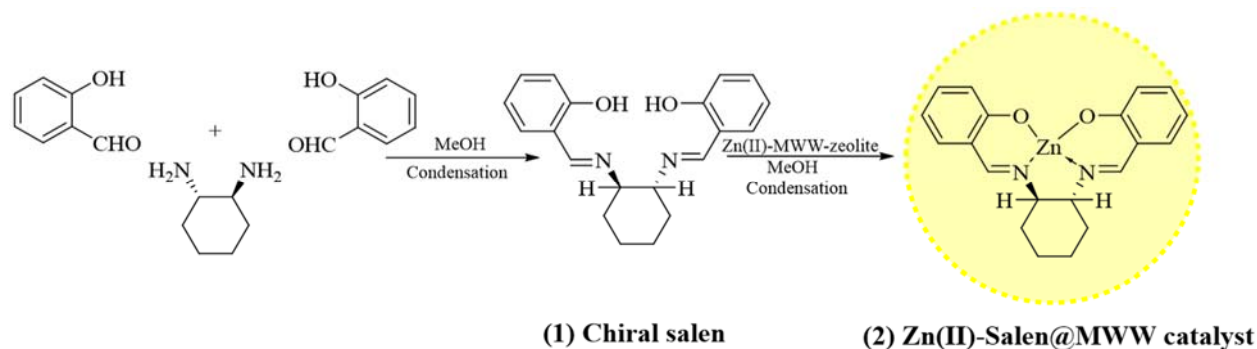
Asymmetric catalysis has become highly advanced in recent years, but there are still challenges to overcome in this area, such as developing environmentally safe methods and using substrates that have been considered unreactive.¹ Ketones, in particular, pose a significant challenge to the current state of asymmetric methodologies.² Due to their low reactivity and difficulties in restraining facial stereoselectivity, some enantioselective chiral catalytic C-C bond formation reactions with carbonyl are available, despite being effective procedures for enantioselective reduction of ketones.³ In contrast, salen-metal complexes may be useful as bifunctional Lewis acid-base catalysts for contemporary catalytic reactions with imperative substrates.⁴

Scientists have embraced the Green Chemistry principles over the past few decades, and environmental considerations have become part of chemical processes.⁵ A significant part of the active pharmaceutical ingredient (API) manufacturing processes relies on the reaction media, which accounts for up to 80% of the total mass.^{6,7} To overcome this issue, the major pharmaceutical companies have developed solvent selection guides for drug synthesis chemical processes. The development of clean technologies that replace hazardous organic solvents with environmentally benign solvents has become progressively popular in recent years.⁸ Owing to this new challenge, organic synthesis has become increasingly popular under solvent-free conditions, as "green chemistry" strives to minimize pollution, costs, and tedious procedures.^{9,10}

In synthetic organic chemistry, multicomponent reactions (MCRs) are becoming increasingly prevalent for their many advantages, including increased atom economy, simplicity, structural disparity, energy savings, and waste reduction.¹¹ MCRs are particularly valuable for the production of distinctly functionalized organic compounds that can succor as valuable heterocyclic forerunners in pharmacology.¹² The Mannich reaction is one such MCR that is widely used for the manufacturing of new-fangled nitrogen-encompassing organic moieties with biological activity.¹³ Aminocarbonyl molecules synthesized through the Mannich reaction can be used as intermediates for the synthesis of many important biomolecules, including amino alcohols, amino acids, peptides, and lactams.¹⁴⁻¹⁹ Among the various Mannich reaction catalytic systems explored,

ultrasonic-assisted organic synthesis (UAOS) is an eco-friendly and competent tactic that significantly enhances reaction rates, yields, and selectivity. In recent years, UAOS has been utilized to uphold multi-component self-Mannich reactions and asymmetric Mannich reactions effectively and expeditiously.^{20–22}

Considering their improved recyclability, novel heterogeneous catalytic systems such as nanoparticle-supported/encapsulated solid acids, metal nanoparticles, and metal-coordinated polymers have received increasing attention in recent years.^{23,24} However, the synthesis of these catalysts limits their practical applications among insoluble bulk materials.^{25–27} As a way to solve this problem, micro- and/or meso- porous siliceous substances like MCM-41, MCM-48, MCM-50, SBA-15, KIT-6, USY zeolite, or MWW-zeolite have been extensively studied because of their unvarying interior pore structure, elevated surface areas, wide-ranging ordered pores with confined size distributions, and superior hydrothermal stability, making them ideal for heterogeneous catalysts. This study uses zinc metal ions as Lewis acids, which are highly potent, low-cost, non-toxic, and soft enough and therefore, suited for Mannich reaction. Herein, we report a green decorum for synthesizing distinctive Zn(II)-Salen ligand encapsulated in MWW host, i.e., Zn(II)-Salen@MWW-zeolite, as a heterogeneous chiral catalyst and employed for the efficient and rapid synthesis of β -amino ketones under measily conditions using an ultrasound-assisted one-pot tactic in solvent-free conditions (*Scheme 5.1*).



Scheme 5.1 A schematic representation of the preparation of chiral salen ligand (1) and Zn(II)-Salen@MWW-zeolite catalyst (2).

5.2 Experimental Section

5.2.1 Synthesis of MWW-zeolites:

Using hexamethyleneimine (HMI) as a template, we synthesized MWW-zeolites using a previously reported protocol.^{28–30}

5.2.2 Preparation of chiral salen ligand:

A chiral salen ligand was prepared from chiral amine and salicylaldehyde using a reported method.^{31–33}

5.2.3 Zn(II) exchanged MWW-zeolite:

A sample was prepared by mixing 5 grams of MWW-zeolite with 12 mmol of zinc acetate salt in 300 ml of deionized water with continuous stirring for 24 hours at 90 °C. As soon as the stirring period ended, the final product was isolated and washed numerous times with deionized water to remove any free metal ions. Following this, the solid was dried at 120 °C for 15 hours.^{34,35}

5.2.4 Synthesis of chiral Zn(II)-Salen@MWW-zeolite:

A Zn(II)-MWW-zeolite, was combined with an excess of chiral salen in a round flask. The ratio of metal to ligand was 0.33. The mixture was covered with an adequate amount of solvent and subjected to reflux for 24 hours under a flow of nitrogen gas. The unbound ligands were eliminated by extracting with acetone, and any free Zn(II) ions that were not coordinated were removed via an ion-exchange process using a 0.1 M sodium chloride solution. Afterwards, the sample was washed with deionized water, followed by air-drying for a duration of 60 minutes. This process led to the encapsulated of a chiral Zn(II)-Salen ligand securely encapsulated into the MWW-zeolite framework. The resulting product is referred as Zn(II)-Salen@MWW-zeolite catalyst (*Scheme 5.1*).^{4,36–40}

5.2.5 Catalytic activity

A mixture of aniline, benzaldehyde, and acetophenone (each of 1 mmol) was combined with 0.05 g Zn(II)-Salen@MWW-zeolite catalyst in a 50 ml RBF. The reaction mixture was subjected to ultrasonic waves using a bath Sonicator. The reaction was allowed to continue for a duration of 120 minutes. Immediately after the accomplishment of the reaction, the solid catalyst was isolated from the crude solution by dissolving it in ethanol. After an exhaustive wash with ethanol, the catalyst was dried under vacuum for reuse purpose.^{21,41,42}

5.3 Results and Discussion

5.3.1 X-ray Diffraction Patterns

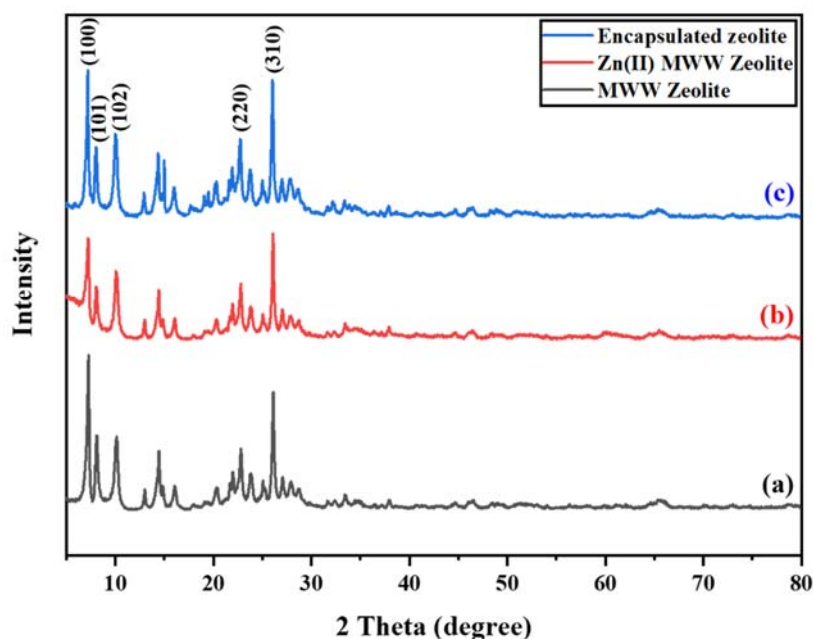


Figure 5.1 XRD patterns of (a) MWW-zeolite (b) Zn(II)-MWW-zeolite (c) chiral Zn-Salen@MWW-zeolite catalyst

Powder X-ray diffraction (XRD) is a crucial technique used to assess the level of crystallinity in powdered samples. *Figure 5.1* displays the XRD patterns of three samples: MWW-zeolite (a), Zn(II)-exchanged MWW-zeolite (b), and chiral Zn-Salen@MWW-zeolite catalyst (c). In all three samples, diffraction peaks are observed at 2θ values of 7.2° , 8.0° , 9.6° , 23° , and 26° , corresponding to the (100), (101), (102), (220), and (310) reflections, respectively. These peaks are distinctive characteristics of the MWW-zeolite. The results ensure that the crystalline arrangement of the MWW-zeolite remains intact after grafting.^{43–46}

5.3.2 Scanning electron microscopy

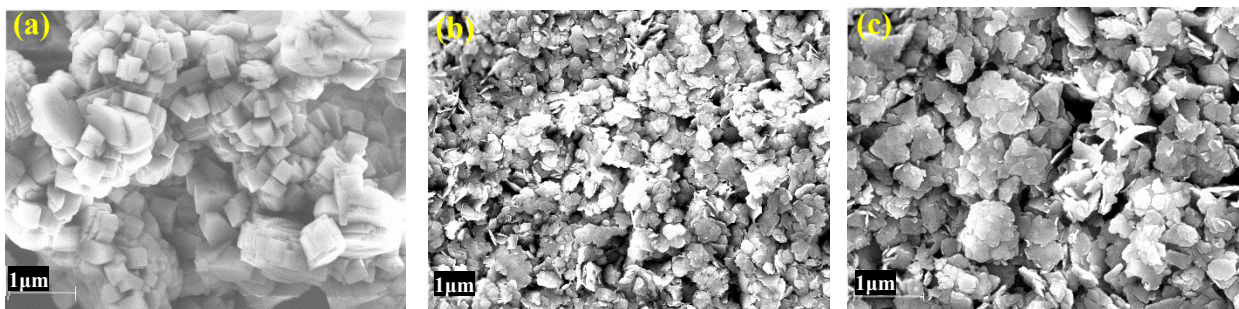


Figure 5.2 FE-SEM results of (a) MWW-zeolite (b) Zn(II)-exchanged MWW-zeolite, (c) chiral Zn-Salen@MWW-zeolite.

In *Figure 5.2* presents FE-SEM images of three samples: MWW-zeolite, Zn(II)-exchanged MWW-zeolite, and chiral Zn-Salen@MWW-zeolite. *Figure 5.2(a)* shows the characteristic cube morphology of the primary crystals of MWW-zeolite. *Figures 5.2(b)* and (c) demonstrate that the introduction of metal and chiral salen scaffold produced minimal alterations in the surface morphology of the MWW-zeolite.^{47–49}

5.3.3 BET analysis

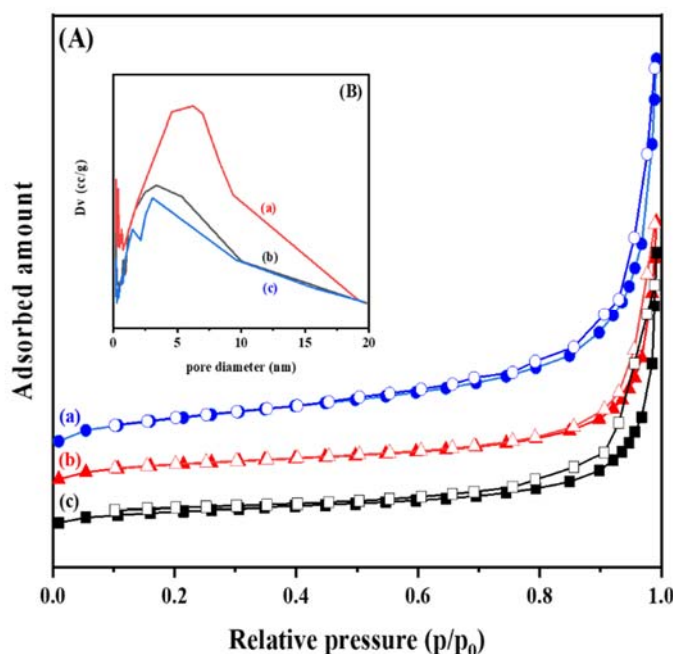


Figure 5.3 (A) N₂ adsorption– desorption isotherms of (a) MWW zeolite (b) Zn(II)-MWW-zeolite and (c) chiral Zn-Salen@MWW-zeolite; (B) BJH pore size distributions of (a) MWW zeolite (b) Zn(II)-MWW zeolite and (c) chiral Zn-Salen@MWW-zeolite.

Table 5.1 Porosity and texture features of catalyst and catalyst precursors

Sample	Surface area/m ² g ⁻¹	Pore volume/cm ³ g ⁻¹	Average pore diameter/nm
MWW-zeolite	414.50	0.51	6.2
Zn(II)-exchanged MWW-zeolite	263.48	0.48	3.3
Chiral Zn(II)-Salen@MWW	31.96	0.14	3.0

Figures 5.3(A) and (B) exhibit N₂ adsorption-desorption isotherms and BJH pore size distributions for MWW-zeolite (a), Zn(II)-exchanged MWW-zeolite (b), and chiral Zn-

Salen@MWW-zeolite (c). The hybrid materials demonstrate consistent pore size distributions within their mesoporous regions due to their type IV isotherm characteristics. These attribute validate the retention of the meticulously arranged mesoporous cage of MWW-zeolite within the synthesized materials. *Table 5.1* presents a decrease in pore diameter, from 6.2 nm in pure MWW-zeolite to approximately 3.3 nm in Zn(II)-exchanged MWW-zeolite and 3.0 nm in chiral Zn(II)-Salen@MWW-zeolite. The BET surface area of the synthesized materials exhibits a gradual reduction, indicating the successful encapsulation of organic scaffolds into the MWW-zeolite.⁵⁰

5.3.4 FTIR spectra

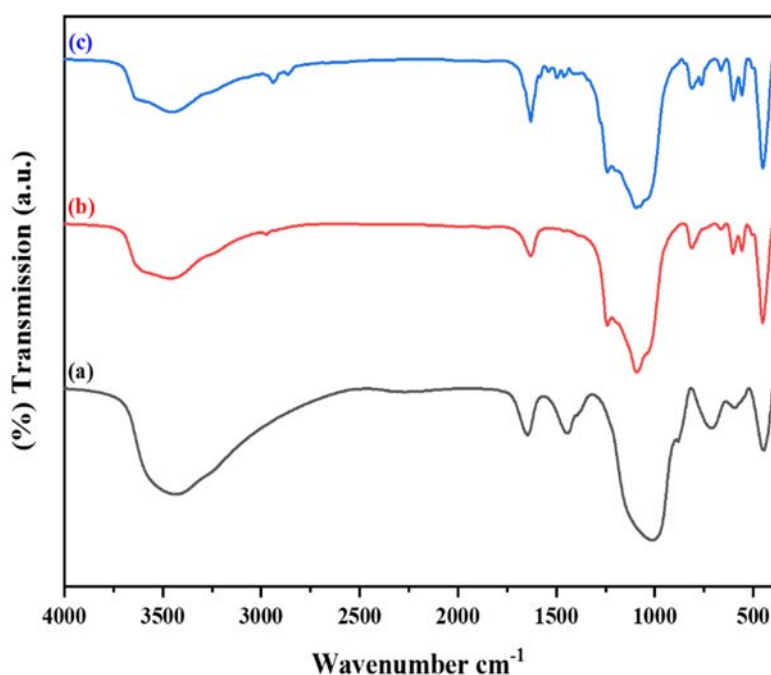


Figure 5.4 FTIR spectra of (a) MWW-zeolite (b) Zn(II)-exchanged MWW-zeolite and (c) chiral Zn(II)-Salen@MWW-zeolite catalyst.

Figure 5.4 illustrates the FTIR spectral data of three samples: MWW-zeolite, Zn(II)-exchanged MWW-zeolite, and chiral Zn(II)-salen@MWW-zeolite. The FTIR spectrum of MWW-zeolite reveals the presence of a prominent and wide band at 1015 cm⁻¹, indicating the occurrence of stretching vibration associated with aluminum silicate element *Figure 5.4(a)*. Conversely, the

IR bands observed in the Chiral Zn(II)-Salen@MWW-zeolite exhibit relatively weak intensities, which could be attributed to the lower concentrations of Zn(II)-Salen present within the cage of MWW-zeolite. However, in the chiral Zn(II)-Salen@MWW-zeolite, this vibration is notably absent, indicating the deprotonation of this group through coordination with the metal ion. In the FTIR spectrum of *Figure 5.4(c)*, the presence of a band at 1629 cm^{-1} ensures that nitrogen interacts with the metal ion. This band shifts to the lower frequency region and observed in the spectra of chiral Zn(II)-Salen@MWW-zeolite. The FTIR spectrum of chiral Zn(II)-Salen complex encapsulated within the MWW-zeolite exhibits a prominent broad band around 3479 cm^{-1} . This specific bands are indicative of -OH stretching, along with relatively less intense band in the range of $804\text{-}816\text{ cm}^{-1}$ for rocking and $664\text{-}694\text{ cm}^{-1}$ wagging vibrations respectively, providing evidence for the presence of lattice water molecules within the framework.⁵¹

5.3.5 EDAX pattern

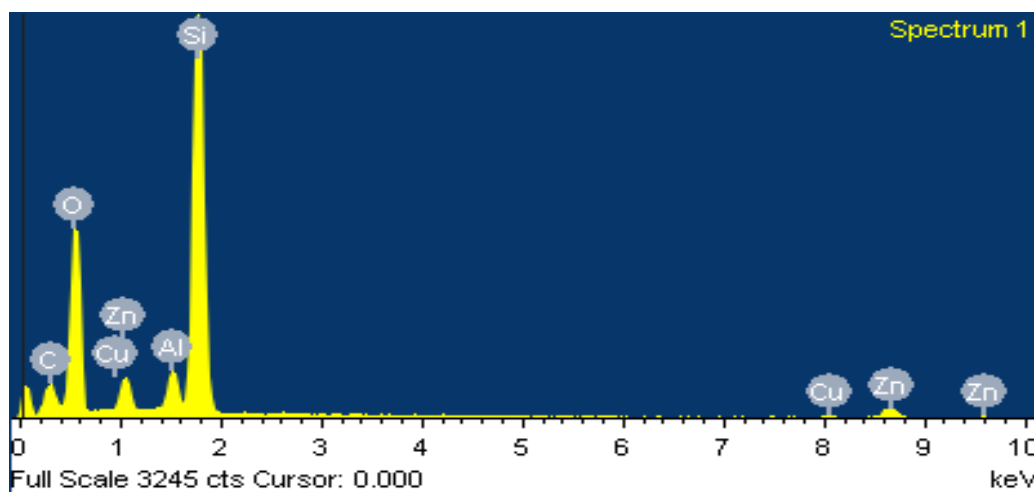


Figure 5.5 EDAX pattern of chiral Zn(II)-Salen@MWW-zeolite catalyst

Figure 5.5 exhibits the results of the EDAX analysis, confirming the existence of Zinc, Silica, Aluminum, and Oxygen elements in the composition of the Chiral Zn(II)-Salen@MWW-zeolite.^{52,53}

5.3.6 X-ray photoelectron spectroscopy

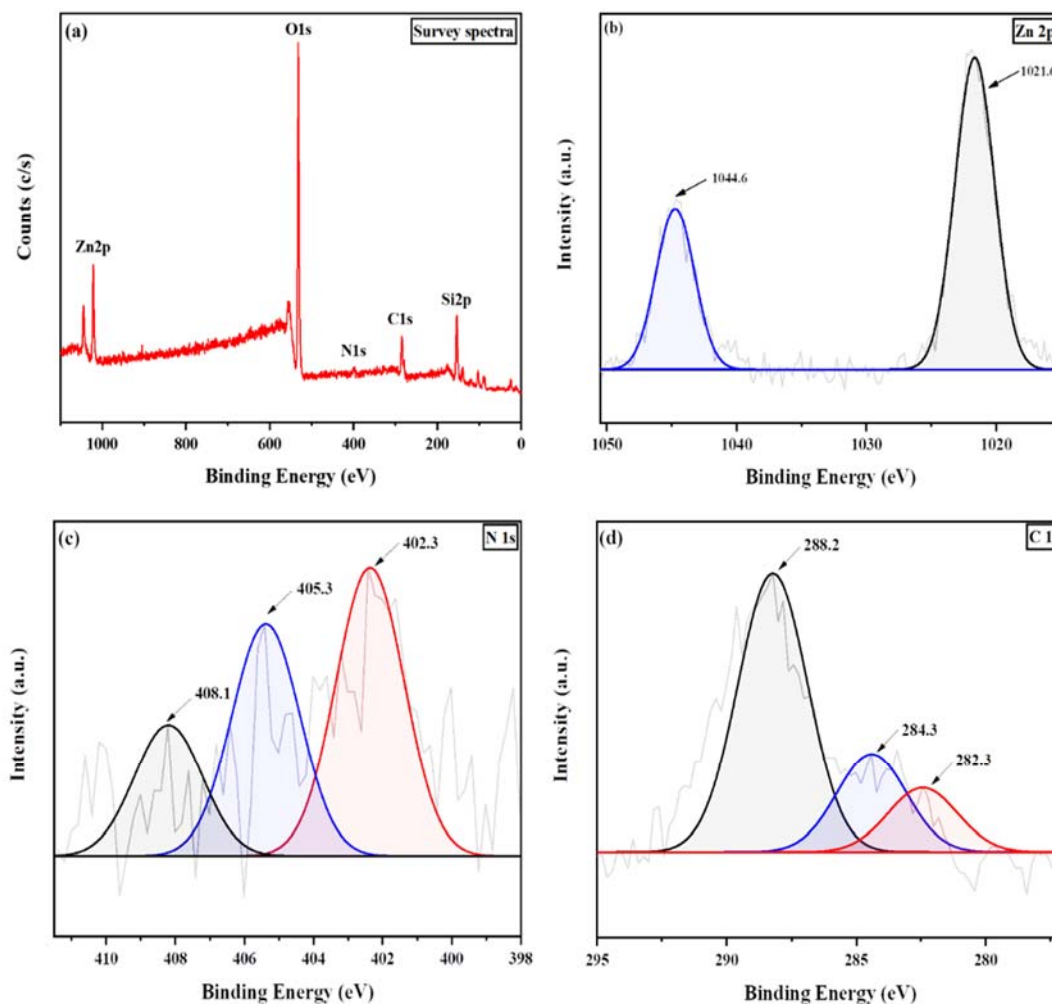


Figure 5.6 XPS spectra of Chiral Zn(II)-Salen@MWW-zeolite; (a) survey spectrum, (b) Zn 2p, (c) N 1s and (d) C 1s.

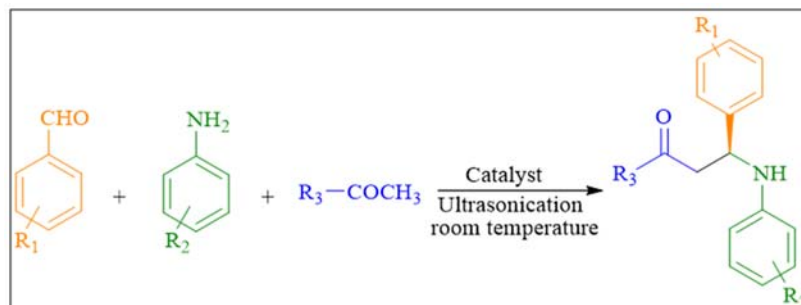
XPS spectra of Chiral Zn(II)-Salen@MWW-zeolite are shown in *Figure 5.6*. This analysis was carried out to examine the surface elemental composition and elemental bonding of the chiral encapsulated Zn(II)-Salen catalyst successfully prepared. The comprehensive XPS spectrum (*Figure 5.6(a)*) demonstrates the existence of Zn, O, Si, C, and N elements. The XPS spectra of Zn 2p (*Figure 5.6(b)*) exhibits two distinctive peaks at 1021.6 eV for Zn 2p_{3/2} and 1044.6 eV for

Zn 2p_{1/2}, confirming the presence of Zn(II) within the sample. In the N 1s spectrum (*Figure 5.6(c)*), three peaks at 402.3 eV (CN), 405.3 eV, and 408.1 eV are observed, indicating the interaction between zinc and nitrogen within the carbon moiety. C 1s spectrum (*Figure 5.6(d)*), exhibits three clearly distinguishable peaks are observed at 282.3 eV, 284.3 eV, and 288.2 eV, which analogous to chemical bonds C-C, C-O or C-N, and C=N, respectively.⁵⁴⁻⁵⁹

5.4 Catalytic activity

As a result of the successful fabrication and characterization of an Chiral Zn(II)-Salen@MWW-zeolite, its catalytic property was assessed for use in one-pot Mannich reaction as shown in *Scheme 5.2*. An environmentally responsible, affordable, long-lasting, and economical reaction route is crucial when it comes to organic transformation reactions. There is one such effective route, i.e., ultrasonic route, which has the advantages of being low energy-consuming, simple to react to, and quick to respond.

Initially, the goal of was to establish an unpretentious method for synthesizing the target product. The use of a catalyst, howbeit, resulted in a higher yield. In ultrasonic-assisted reactions, ultrasonic radiation interacts with the organic substrate, creating transient cavities that are filled with liquid vapour or air. These cavities collapse rapidly after a few ultrasound cycles, generating hot spots with high temperatures and pressures that help break chemical bonds and increase the yield of the product in less time. Through this process, mass flow mechanical energy is transformed into kinetic energy generated by arbitrary molecular translation and rotation. The method is advantageous because it eliminates the need for solvents, which can be associated with complex work-up procedures, safety concerns, high costs, and environmental problems.

5.4.1 Synthesis chiral β -aminoketone derivatives

Scheme 5.2 Synthesis of chiral β -aminoketone derivatives using chiral Zn(II)-Salen@MWW-zeolite.

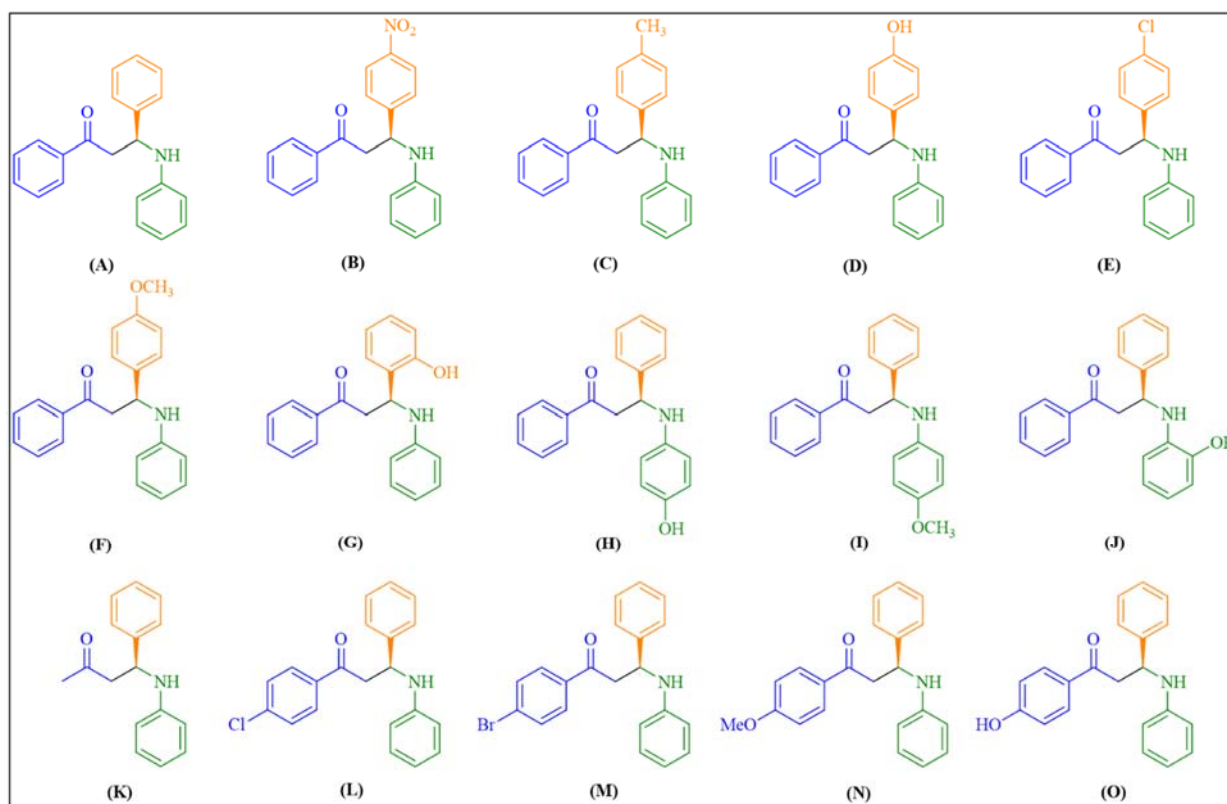


Figure 5.7 Encapsulated chiral Zn(II)-salen complex catalyzes the synthesis of Mannich bases (A-O) derived from aryl ketone. Where aldehyde/aniline/aryl ketone are in a 1:1:1 molar ratio.

To optimize the reaction conditions, we tested varied ratios of starting substrates and found that using 1 mmol of each substrate with a 1:1:1 ratio resulted in a high product yield. With optimized reaction conditions, we synthesized different derivatives of β -amino carbonyl compounds (*Table 5.2*) to evaluate our catalyst's efficiency and performance. We also tested the upshot of substituents in aromatic aldehyde and aniline on product yield. In contrast to aldehydes with electron-donating substituents, those with electron-withdrawing groups produced a greater yield in fewer hours.

Table 5.2 Chiral β -aminoketone derivatives synthesized through the one pot Mannich reaction with diverse substrates employing chiral Zn(II)-Salen@MWW-zeolite catalyst

Entry	Substrates (R ₁ , R ₂ and R ₃)	Product ^a	Conversion (%)	ee (%) ^b
1	R ₁ = H; R ₂ = H; R ₃ = -Ph	A	94	94.58
2	R ₁ = 4-NO ₂ ; R ₂ = H; R ₃ = -Ph	B	96	96.33
3	R ₁ = 4-Me; R ₂ = H; R ₃ = -Ph	C	95	95.40
4	R ₁ = 4-OH; R ₂ = H; R ₃ = -Ph	D	88	89.73
5	R ₁ = 4-Cl; R ₂ = H; R ₃ = -Ph	E	93	89.45
6	R ₁ = 4-OMe; R ₂ = H; R ₃ = -Ph	F	89	88.00
7	R ₁ = 2-OH; R ₂ = H; R ₃ = -Ph	G	81	84.07
8	R ₁ = H; R ₂ = 4-OH; R ₃ = -Ph	H	87	91.82
9	R ₁ = H; R ₂ = 4-OMe; R ₃ = -Ph	I	88	89.58
10	R ₁ = H; R ₂ = 2-OH; R ₃ = -Ph	J	80	83.72
11	R ₁ = H; R ₂ = H; R ₃ = -CH ₃	K	95	94.35
12	R ₁ = H; R ₂ = H; R ₃ = 4-Cl-Ph	L	95	89.95
13	R ₁ = H; R ₂ = H; R ₃ = 4-Br-Ph	M	93	88.96
14	R ₁ = H; R ₂ = H; R ₃ = 4-OMe-Ph	N	86	87.67
15	R ₁ = H; R ₂ = H; R ₃ = 4-OH-Ph	O	84	86.98

^a As shown in *Figure 5.7*; ^b ee analyzed through chiral HPLC; Reaction conditions: mole ratio of aldehydes, amine and ketone (1:1:1), and chiral Zn(II)-Salen@MWW-zeolite (0.05 g), ultrasonication, 120 min.

The products obtained were thoroughly analyzed through chiral HPLC and confirmed by FTIR, ¹H & ¹³C NMR spectroscopy, and their data were compared with previously reported data. In addition to the synergistic effect among the individual components, the chiral Zn(II)-Salen surface was able to adsorb significant amounts of reactant molecules, increasing its catalytic activity. Considering the above results, the presence of Brønsted and Lewis acidic sites, the synergistic effect amid the discrete components, and the larger surface area of the catalyst play crucial roles in its altogether catalytic performance. The activation of the reaction was further facilitated by ultrasonic wave through the preparation of β -amino carbonyl compounds.

5.4.2 Recyclability test

The catalyst's recyclability and stability are crucial for its effectiveness. To investigate this, we used the optimized conditions to assess the catalyst's reusability. As soon as the reaction was completed, the catalyst was recovered, washed with ethyl acetate to remove organic parts, and dried for 3 hours underneath vacuum at 80°C. Despite reusing the chiral Zn(II)-Salen@MWW-zeolite catalyst five times, we observed only petite losses in catalytic activity. The fresh sample yielded 94% product yield and 94.58% ee as the catalytic run was being carried out, but these numbers somewhat fell to 85% and 82.44%, respectively, after the fifth run, as stated in *Table 5.3* and their bar chart, which is depicted in *Figure 5.8*.

Table 5.3 Recyclability data of the chiral β -aminoketone derivatives synthesis

Entry	Conversion (%)	ee (%) ^a
1	94	94.58
2	91	92.98
3	89	87.83
4	86	83.91
5	85	82.44

^a ee analyzed through chiral HPLC; Reaction conditions: mole ratio of aldehydes, amine and ketone (1:1:1), and chiral Zn(II)-Salen@MWW-zeolite (0.05 g), ultrasonication, 120 min.

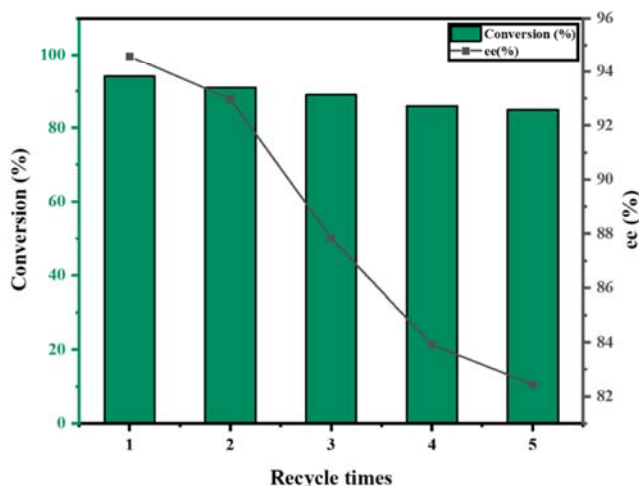


Figure 5.8 Recyclability test of chiral Zn(II)-Salen@MWW-zeolite catalyst over chiral β -aminoketones synthesis.

5.4.3 A comparative study for the synthesis of chiral β -aminoketone

Table 5.4 presents a comparison of chiral catalytic systems, both heterogeneous and homogeneous, utilized in chiral β -aminoketone synthesis. The results reveal that the present catalyst was compared to other previously reported catalysts and showed superior efficiency using a sustainable ultrasonic method, demonstrating higher activity within a short time frame.^{13,60–66}

Table 5.4 A comparative study for the synthesis of the chiral β -aminoketone derivatives

Entry	Catalyst	Yield (%)	Time (hours)	Amount of catalyst (mol %)	Reference
1	H ₃ PW ₁₂ O ₄₀	89	18	0.24	[15]
2	sucrose char sulfonic acid	91	10	4	[18]
3	NH ₂ SO ₃ H	94	1.5	10	[22]
4	Hf(OTf) ₄	89	6	5	[53]
5	NDPANI	94	7	4	[55]

5.5 A plausible reaction pathway for the chiral β -aminoketone derivatives synthesis

Considering all the above results, a plausible mechanism has been proposed and is presented in *Figure 5.5*. As a result of the acidic nature of the catalyst (Brønsted as well as Lewis) and the effective adhesion of reactant molecules to its surface, the reaction begins under ultrasonic irradiation. During the reaction, the carbonyl group of the aldehyde substrate is activated by protonation (predominantly by the acidic Brønsted sites of the active catalyst), while the Lewis acidic site activates aniline substrate. In the next step, the activated aldehyde is dehydrated by the nucleophilic aniline in order to form an iminium intermediate.

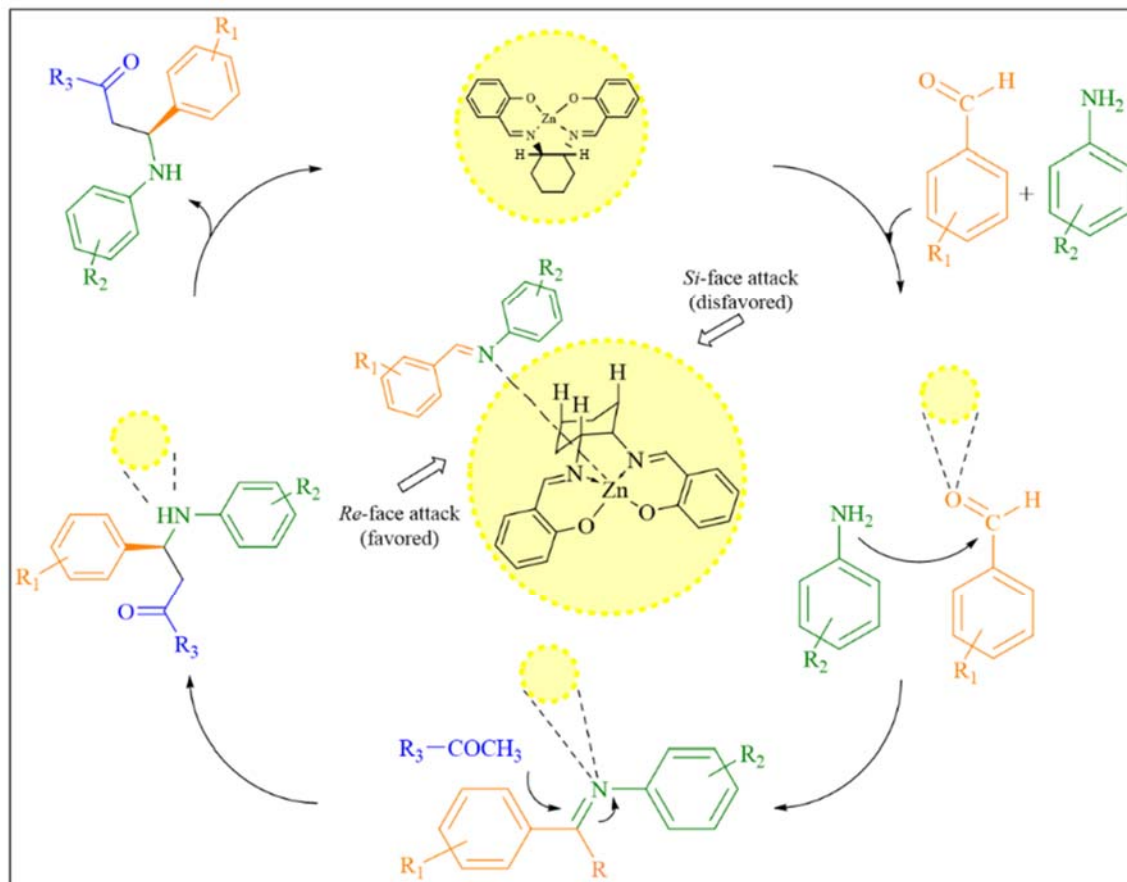


Figure 5.5 A plausible reaction pathway for the chiral β -aminoketone derivatives synthesis and transition state models for the prediction of stereoselectivity

The asymmetric Mannich reaction of iminium intermediate with ketone had previously been reported to generate *in-situ* metal complexes through axially chiral salen ligands (Figure 5.5). These transition states readily explain the observed *Re*-facial enantioselectivity is favored and the opposite selectivity (*Si*) is disfavored.⁴

Moreover, the desired product was efficiently produced by generating cavitation through ultrasonic irradiation. This process involved the formation and collapse of microbubbles, generating an enormous amount of thermal energy and district pressure that facilitated the fabrication of β -amino carbonyl compounds. The presence of acid groups on the catalyst, along with ultrasonic irradiation, favoured the dehydration process during the formation of the

intermediate. Prior literature has referred to an analogous mechanism involving metal nanoparticles for the synthesis of β -aminocarbonyl compounds.

5.6 Conclusion

In this study, a highly persuasive, unprecedented and atypical encapsulated chiral Zn(II)-Salen catalyst, Zn(II)-Salen@MWW-zeolite, was fabricated, characterized, and used to synthesize chiral β -amino carbonyls via a one-pot three-component using an ultrasonic irradiation. Related to other reported systems, the present catalyst demonstrated superior performance with a higher product yield of 94 % and 94.58 ee (%) selectivity achieved in a shorter reaction time (120 min). Furthermore, the existence of acidic sites, a sky-scraping the area of surface, ultrasonic irradiation, and cooperative interaction among the discrete parts contribute to increased activity. Moreover, the catalyst exhibited remarkable reusability for up to five consecutive cycles, maintaining significant catalytic performance without substantial degradation. In summary, this study demonstrates that encapsulating chiral metal salen ligands on acidic zeolite surfaces can lead to highly effective, durable, and recyclable catalysts for various organic transformations.

5.7 References

1. Nicolaou, K. C., Zhong, Y.-L., & Baran, P. S. A new method for the one-step synthesis of α,β -unsaturated carbonyl systems from saturated alcohols and carbonyl compounds. *J. Am. Chem. Soc.* **2000**, 122, 7596-7597.
2. Lakhani, P. & Modi, C. K. Shaping enantiochemistry : Recent advances in enantioselective reactions via heterogeneous chiral catalysis. *Mol. Catal.* **2023**, 548, 113429.
3. Petrovic, V. P., Petrovic, V. P. & Petrovic, Z. D. Acetophenone Mannich bases : study of ionic liquid catalysed synthesis and antioxidative potential of products. *R. Soc. open sci.* **2018**, 5, 181232.
4. Shaw, S. & White, J. D. Asymmetric Catalysis Using Chiral Salen-Metal Complexes: Recent Advances. *Chem. Rev.* **2019**, 119, 9381–9426.
5. Alfonsi, K. *et al.* Green chemistry tools to influence a medicinal chemistry and research chemistry based organisation. *Green Chem.* **2008**, 10, 31-36.

6. Henderson, R. K., Jiménez-González, C., Constable, D. J. C., Alston, S. R., Inglis, G. G. A., Fisher, G., Sherwood, J., Binks, S. P., & Curzons, A. D. Green Chemistry Expanding GSK's solvent selection guide— embedding sustainability into solvent selection starting at medicinal chemistry. *Green Chem.* **2011**, 13, 854–862.
7. David J. C. Constable, Conchita Jimenez-Gonzalez, & Richard K. Henderson. Perspective on Solvent Use in the Pharmaceutical Industry. *Org. Process Res. Dev.* **2007**, 11, 1, 133–137.
8. Shamna S., Afsina C. M. A., & Philip M., Recent advances and prospects in the Zn-catalysed Mannich reaction. *RSC Adv.*, **2021**, 11, 9098.
9. Lakhani P., *et al.* DFT stimulation and experimental insights of chiral Cu(II)-salen scaffold within the pocket of MWW-zeolite and its catalytic study. *Phys. Chem. Chem. Phys.*, **2023**, 25, 14374-14386.
10. Da Silveira, R. G. Synthesis, Structure Determination and Catalytic Activity of a Novel Ruthenium(II) [RuCl(dppb)(44bipy)(4-pic)]PF₆ Complex. *J. Braz. Chem. Soc.* **2021**, 32, 1802–1812.
11. Rotstein, B. H., Zaretsky, S., Rai, V. & Yudin, A. K. Small heterocycles in multicomponent reactions. *Chem. Rev.* **2014**, 114, 8323–8359.
12. Verkade, J. M. M., Hemert, L. J. C. Van, Quaedflieg, J. L. M. & Rutjes, F. P. J. T. Organocatalysed asymmetric Mannich reactions. *Chem. Soc. Rev.* **2008**, 37, 29-41.
13. Kumar, A., Gupta, M. K. & Kumar, M. Green Chemistry catalysed multicomponent synthesis of 3-amino alkylated indoles via a Mannich-type reaction under solvent-free conditions. *Green Chem.* **2012**, 14, 290-295.
14. Kumar, A., Gupta, M. K. & Kumar, M. An efficient non-ionic surfactant catalyzed multicomponent synthesis of novel benzylamino coumarin derivative via Mannich type reaction in aqueous media. *Tetrahedron Lett.* **2011**, 52, 4521–4525.
15. Azizi, N., Torkiyan, L. & Saidi, M. R. Highly Efficient One-Pot Three-Component Mannich Reaction in Water Catalyzed by Heteropoly Acids. *Org. Lett.*, **2006**, 8, 10.
16. Azizi, N., Baghi, R., Batebi, E. & Bolourtchian, S. M. Catalytic stereoselective Mannich reaction under solvent-free conditions *C. R. Chim.*, **2012**, 15, 278–282.
17. Iwanejko, J., Wojaczyńska, E. & Olszewski, T. K. Green chemistry and catalysis in Mannich reaction. *Curr. Opin. Green Sustain. Chem.*, **2018**, 10, 27-34.

18. Xu, Q., Yang, Z., Yin, D. & Wang, J. One-pot three-component Mannich reaction catalyzed by sucrose char sulfonic acid. *Front. Chem. Eng. China.*, **2009**, 3(2), 201–205.
19. Yonghai H., Wei S., Xie S., Wang C., Zhengfeng X., Three-Component Mannich Reaction Catalyzed by MCM-41 Immobilized H₃PW₁₂O₄₀ (PW) in Water. *Chinese J. Org. Chem.* **2014**, 34, 1212-1217.
20. Ozturkcan S. Arda, Turhan K., Turgut Z. Ultrasound-assisted rapid synthesis of β -aminoketones with direct-type catalytic Mannich reaction using bismuth(III)triflate in aqueous media at room temperature. *Chem. Pap.* **2012**, 66 (1), 137-147.
21. L. Achary S. K., Nayak P. S., Barik B., Kumar A., Dash P., Ultrasonic-assisted green synthesis of β -amino carbonyl compounds by copper oxide nanoparticles decorated phosphate functionalized graphene oxide via Mannich reaction. *Catal. Today* **2020**, 348, 137-147
22. Zeng, H., Li, H. & Shao, H. Ultrasonics Sonochemistry One-pot three-component Mannich-type reactions using Sulfamic acid catalyst under ultrasound irradiation. *Ultrason-Sonochemistry.* **2009** 16, 758–762.
23. Lakhani, P. & Modi, C. K. Spick-and-span protocol for designing of silica-supported enantioselective organocatalyst for the asymmetric aldol reaction. *Mol. Catal.*, **2022** 525 112359.
24. Lakhani, P. & Modi, C. K.. Asymmetric Hydrogenation using Covalently Immobilized Ru-BINOL-AP@MSNs Catalyst. *New J. Chem.*, **2023** 47, 8767–8775.
25. Chu, W. Effect of Binder Type on MWW-Based Catalysts for the Liquid-Phase Alkylation Reaction of Benzene with Ethylene. *Ind. Eng. Chem. Res.* **2022**, 61, 2693–2700.
26. Jin, S. A facile organosilane-based strategy for direct synthesis of thin MWW-type titanosilicate with high catalytic oxidation performance. *Catal. Sci. Technol.* **2018**, 8, 6076–6083.
27. Zhou, Y. Enhanced Surface Activity of MWW Zeolite Nanosheets Prepared via a One-Step Synthesis. *J. Am. Chem. Soc.* **2020**, 142, 8211–8222.
28. Ahmad, A., Naqvi, S. R., Rafique, M., Nasir, H. & Sarosh, A. Synthesis, characterization and catalytic testing of MCM-22 derived catalysts for n-hexane cracking. *Sci. Rep.* **2020**, 10, 1–11.
29. Schwanke, A. & Pergher, S. Lamellar MWW-type zeolites: Toward elegant nanoporous

- materials. *Appl. Sci.* **2018**, 8, 1636.
30. Jakkidi Krishna Reddy, Kshudiram Mantri, Shruti Lad, Jagannath Das, Ganesan Raman, Raksh vir Jasra. Synthesis of Ce-MCM-22 and its enhanced catalytic performance for the removal of olefins from aromatic stream. *J. Porous Mater.* **2020**, 27, 1649–1658.
 31. Shiryaev, A. A. A chiral (1R,2R)-N,N'-bis-(salicylidene)-1,2-diphenyl-1,2-ethanediamine Schiff base dye: synthesis, crystal structure, Hirshfeld surface analysis, computational study, photophysical properties and in silico antifungal activity. *J. Iran. Chem. Soc.* **2021**, 18, 2897–2911.
 32. Baleizão, C. & Garcia, H. Chiral salen complexes: An overview to recoverable and reusable homogeneous and heterogenous catalysts. *Chem. Rev.* **2006**, 106, 3987–4043.
 33. Yuan, G., Jiang, H., Zhang, L., Liu, Y. & Cui, Y. Metallosalen-based crystalline porous materials: Synthesis and property. *Coord. Chem. Rev.* **2019**, 378, 483–499.
 34. Motokura, K., Ding, S., Usui, K. & Kong, Y. Enhanced Catalysis Based on the Surface Environment of the Silica-Supported Metal Complex. *ACS Catal.* **2021**, 11, 11985–12018.
 35. Modi, C. K., Trivedi, P. M., Gupta, S. K. & Jha, P. K. Transition metal complexes enslaved in the supercages of zeolite-Y: DFT investigation and catalytic significance. *J. Incl. Phenom. Macrocycl. Chem.* **2012**, 74, 117–127.
 36. Uhrmacher, F., Elbert, S. M., Rominger, F. & Mastalerz, M. Synthesis of Large [2+3] Salicylimine Cages with Embedded Metal-Salphen Units. *Eur. J. Inorg. Chem.* **2022**, 2022, 1–9.
 37. Kargar, H. Synthesis, spectral characterization, and theoretical investigation of Ni(II) and Pd(II) complexes incorporating symmetrical tetradentate Schiff base ligand: Suzuki-Miyaura cross-coupling reaction using PdLSym. *J. Iran. Chem. Soc.* **2022**, 19, 3981–3992.
 38. Yimthachote, S., Chumsaeng, P. & Phomphrai, K. Complexity of imine and amine Schiff-base tin(ii) complexes: Drastic differences of amino and pyridyl side arms. *Dalt. Trans.* **2022**, 51, 509–517.
 39. Yuan, Y. C., Mellah, M., Schulz, E. & David, O. R. P. Making Chiral Salen Complexes Work with Organocatalysts. *Chem. Rev.* **2022**, 122, 8841–8883.
 40. Gbery, G., Zsigmond, A. & Balkus, K. J. Enantioselective epoxidations catalyzed by zeolite MCM-22 encapsulated Jacobsen's catalyst. *Catal. Letters* **2001**, 74, 77–80.
 41. List B. The Direct Catalytic Asymmetric Three-Component Mannich Reaction. *J. Am.*

- Chem. Soc.* **2000**, 122, 38, 9336–9337
42. Longo L. S., & Craveiro, M. V. Deep Eutectic Solvents as Unconventional Media for Multicomponent Reactions. *J. Braz. Chem. Soc.* **2018**, 29, 1999–2025.
 43. Moezzi, A., Cortie, M. B. & Mcdonagh, A. M. Zinc hydroxide sulphate and its transformation to crystalline zinc oxide. *Dalton Trans.* **2013**, 42, 14432-14437.
 44. Kazemi, A., Salavati-niasari, M. & Khansari, A. Solvent-less synthesis of zinc oxide nanostructures from Zn (salen) as precursor and their optical properties *Particuology* Solvent-less synthesis of zinc oxide nanostructures from Zn (salen) as precursor and their optical properties. *Particuology* **2012**, 10, 759–764.
 45. Cao, S., Shang, Y., Liu, Y., Wang, J., Sun, Y., Gong, Y., Mo, G., Li, Z., & Liu, P. “Desert Rose” MCM-22 microsphere: Synthesis, formation mechanism and alkylation performance. *Microporous Mesoporous Mater.* **2021**, 315, 110910.
 46. Thakkar, R. & Bandyopadhyay, R. Preparation, characterization, and post-synthetic modification of layered MCM-22 zeolite precursor. *J. Chem. Sci.* **2017**, 129, 1671–1676.
 47. Juneau, M. *et al.* Characterization of Metal-zeolite Composite Catalysts: Determining the Environment of the Active Phase. *ChemCatChem* **2020**, 12, 1826–1852.
 48. Chen, J. Catalytic performances of cu/mcm-22 zeolites with different cu loadings in nh₃-scr. *Nanomaterials* **2020**, 10, 1–20.
 49. Srilai, S. Synthesis of zeolite A from bentonite via hydrothermal method: The case of different base solution. *AIP Conf. Proc.* **2020**, 2279, 060006.
 50. Yang, Y., Zhang, Y., Hao, S. & Kan, Q. Tethering of Cu(II), Co(II) and Fe(III) tetrahydro-salen and salen complexes onto amino-functionalized SBA-15: Effects of salen ligand hydrogenation on catalytic performances for aerobic epoxidation of styrene. *Chem. Eng. J.* **2011**, 171, 1356–1366.
 51. Modi, C. K. & Trivedi, P. M. Zeolite-Y based nanohybrid materials: Synthesis, characterization and catalytic aspects. *Microporous Mesoporous Mater.* **2012**, 155, 227–232.
 52. Carriço, C. S. MWW-type catalysts for gas phase glycerol dehydration to acrolein. *J. Catal.* **2016**, 334, 34–41.
 53. Kianfar, A. H., Tavanapour, S., Eskandari, K., Azarian, M. H., Mahmood, W. A. K., & Bagheri, M. Experimental and theoretical structural determination, spectroscopy and

- electrochemistry of cobalt (III) Schiff base complexes: immobilization of complexes onto Montmorillonite-K10 nanoclay. *J. Iran. Chem. Soc.* **2018**, 15, 369–380.
54. Sun, J., Fan H., Nan B., & Ai, S. Fe₃O₄@LDH@Ag/Ag₃PO₄ submicrosphere as a magnetically separable visible-light photocatalyst **2014**, 130, 84-90.
55. Khalid, A. Enhanced Optical and Antibacterial Activity of Hydrothermally Synthesized Cobalt-Doped Zinc Oxide Cylindrical Microcrystals. *Materials*, **2021**, 14(12), 3223
56. Claros, M., Setka, M., Jimenez, Y. P. & Vallejos, S. AACVD Synthesis and Characterization of Iron and Copper Oxides Modified ZnO Structured Films. *Nanomaterials*, **2020**, 10(3), 471.
57. Abd El Khalk, A. A., Betiha, M. A., Mansour, A. S., Abd El Wahed, M. G. & Al-Sabagh, A. M. High Degradation of Methylene Blue Using a New Nanocomposite Based on Zeolitic Imidazolate Framework-8. *ACS Omega* **2021**, 6, 26210–26220.
58. Vithalani, R. S., Patel, D., Modi, C. K., Jha, P. K., Srivastava, H., & Kane, S. R. Synthesis of less acidic VO-salen complex grafted onto graphene oxide via functionalization of surface carboxyl groups for the selective oxidation of norbornene. *Graphene Technol.* **2020**, 5, 83–101.
59. Chao, S. Nitrogen-doped Carbon Derived from ZIF-8 as a High-performance Metal-free Catalyst for Acetylene Hydrochlorination. *Sci. Rep.* **2017**, 7, 1–7.
60. Gil-ord, M., Aubry, C., Niño, C. & Maestro, A., Andrés J. M., Squaramide-Catalyzed Asymmetric Mannich Reaction between 1,3-Dicarbonyl Compounds and Pyrazolinone Ketimines: A Pathway to Enantioenriched 4-Pyrazolyl- and 4-Isoxazolyl-4-aminopyrazolone Derivatives. *Molecules*, **2022**, 27(20), 6983
61. Han, S., Wei, J., Peng, X., Liu, R. & Gong, S. Hf(OTf)₄ as a Highly Potent Catalyst for the Synthesis of Mannich Bases under Solvent-Free Conditions. *Molecules*. **2020**, 25(2), 388
62. Kiani M., Anaraki-Ardakani H., Hasanzadeh N. & Rayatzadeh A. Fe₃O₄@saponin/Cd: a novel magnetic nano-catalyst for the synthesis of β-aminoketone derivatives. *J. Iran. Chem. Soc.* **2020**, 17, 2243–2256.
63. Behera S., Patra B. N. One-pot synthesis of β-amino carbonyl compounds under solvent free condition by using alum doped nanopolyaniline catalyst. *Polymer* **2021**, 228 123851.
64. Saikia, S., Gogoi, P., Dutta, A. K., Sarma, P. & Borah, R. Chemical Design of multifaceted acidic 1, 3-disulfoimidazolium chlorometallate ionic systems as heterogeneous catalysts for

- the preparation of β -amino carbonyl compounds. *Journal Mol. Catal. A, Chem.* **2016**, 416, 63–72.
65. Azizi N. & Edrisi M. Deep eutectic solvent immobilized on SBA-15 as a novel separable catalyst for one-pot three-component Mannich reaction. *Microporous Mesoporous Mater.* **2016**, 240, 130-136.
66. Ganwir, P. & Chaturbhuj, G. U. Aluminized Polyborate : A New and Eco-friendly Catalyst for One-pot Multicomponent Synthesis of Reaction. *Org. Prep. Proced. Int.* **2022**, 54, 338–345.